Supporting Information

Excimer formation effects and trap-assisted charge recombination loss channels in organic solar cells of perylene diimide dimer acceptors

Ranbir Singh [a, b], Min Kim [a], Jae-Joon Lee [b], Tengling Ye [c], Panagiotis E. Keivanidis [d, *], Kilwon Cho [a]

[a] Department of Chemical Engineering, Pohang University of Science and Technology, Pohang, 790−784, Korea

[b] Department of Energy & Materials Engineering, Dongguk University, Seoul 04620, Republic of Korea

[c] MIIT Key Laboratory of Critical Materials Technology for New Energy Conversion and Storage, School of Chemistry and Chemical Engineering, Harbin Institute of Technology, Harbin, China

[d] Device Technology and Chemical Physics Lab, Department of Mechanical Engineering and Materials Science and Engineering, Cyprus University of Technology, Limassol 3041, Cyprus

non-geminate recombination; fullerene-free solar cells; charge trapping; multiple-diode electrical equivalent circuit; configurational conformation

[*]Asst. Prof. Panagiotis E. Keivanidis, p.keivanidis@cut.ac.cy
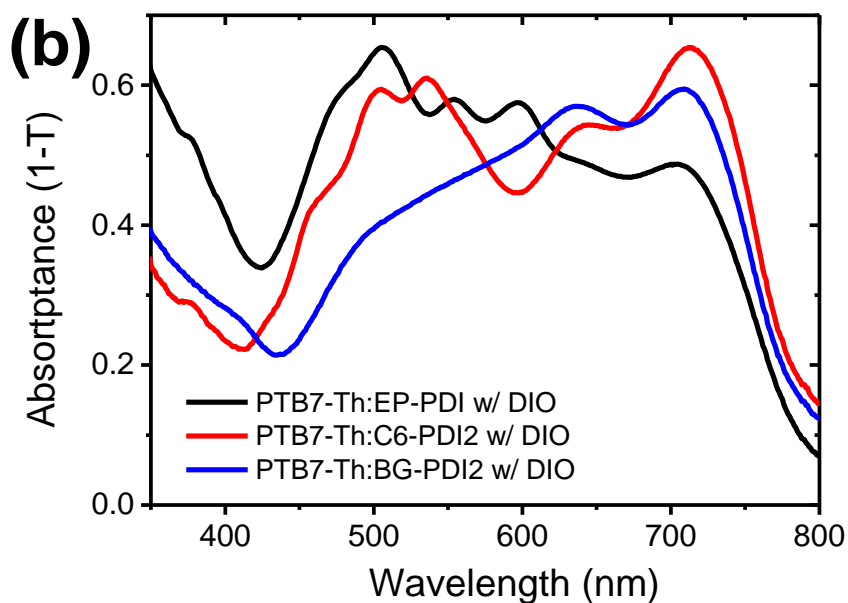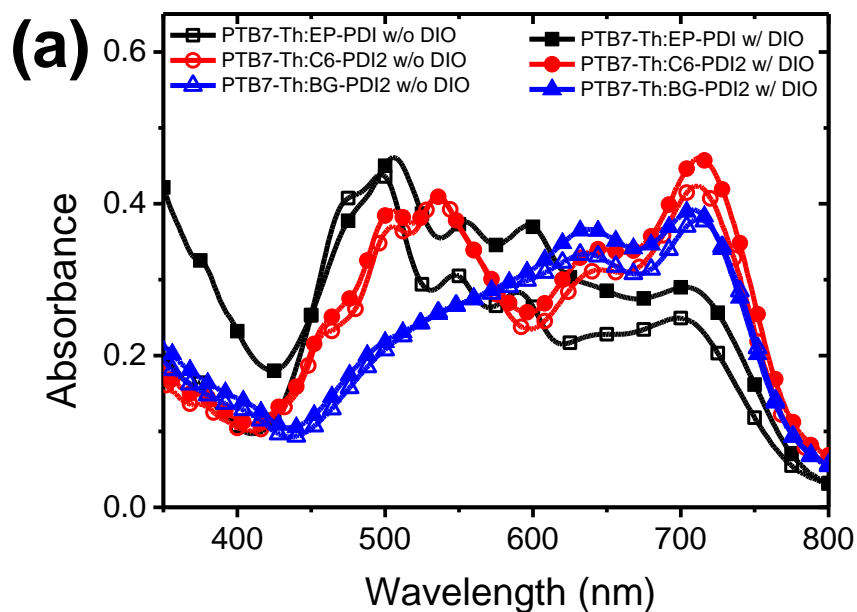
Fig. S1 a) Absorption spectra of PTB7-Th:EP-PDI, PTB7-Th:C6-PDI2 and PTB7-Th:BG-PDI2 blend films without (w/o) and with (w/) DIO. b) Absorptance (1-T) spectra of PTB7-Th:EP-PDI, PTB7-Th:C6-PDI2 and PTB7-Th:BG-PDI2 blend films with (w/) DIO.
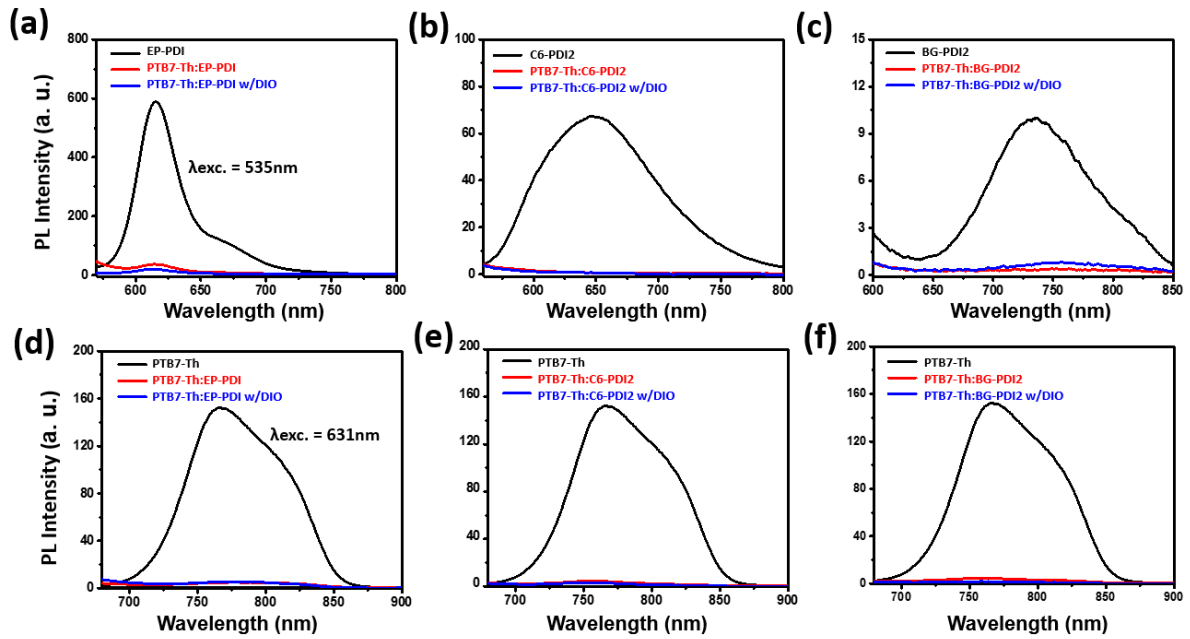
Fig. S2 PL quenching spectra of the PTB7-Th:EP-PDI, PTB7-Th:C6-PDI2 and PTB7-Th:BG-PDI2 blend films with and without DIO w.r.t. pristine film (a-c) EP-PDI, C6-PDI2 and BG-PDI2, and (d-f) PTB7-Th, respectively, where all the films were excited at (a-c) 535 nm and (d-f) 631nm wavelength.

Table S2 Photovoltaic performances of solar cells based on PTB7-Th:EP-PDI, PTB7-Th:C6-PDI2 and PTB7-Th:BG-PDI2 photoactive layers, with different concentration of DIO additive content (simulated solar illumination conditions AM 1.5G illumination, 100 mW cm^{-2}). The $PCE_{av.}$ values correspond to averaged PCE as obtained from six devices.

System	V_{OC} (V)	J_{SC} (mA cm^{-2})	FF (%)	$PCE_{av.(max)}$ (%)
PTB7-Th:EP-PDI	0.82 ± 0.01	6.68 ± 0.08	44.7 ± 1.12	2.54 (2.62)
PTB7-Th:EP-PDI + 0.5% DIO*	0.81 ± 0.01	8.04 ± 0.18	55.5 ± 1.08	3.54 (3.65)
PTB7-Th:C6-PDI2	0.78 ± 0.01	11.17 ± 0.12	50.1 ± 0.63	4.56 (4.78)
PTB7-Th:C6-PDI2 + 1.0% DIO*	0.76 ± 0.005	12.47 ± 0.16	55.8 ± 0.79	5.25 (5.36)
PTB7-Th:BG-PDI2	0.90 ± 0.01	7.84 ± 0.07	40.7 ± 1.01	2.82 (3.04)
PTB7-Th:BG-PDI2 + 2% DIO	0.89 ± 0.07	8.27 ± 0.15	46.3 ± 0.98	3.29 (3.42)
PTB7-Th:BG-PDI2 + 3% DIO	0.88 ± 0.06	8.46 ± 0.09	47.8 ± 1.01	3.46 (3.62)
PTB7-Th:BG-PDI2 + 4% DIO	0.88 ± 0.01	8.63 ± 0.18	48.6 ± 1.13	3.84 (4.12)
PTB7-Th:BG-PDI2 + 5% DIO	0.88 ± 0.009	8.52 ± 0.11	45.5 ± 0.86	3.41 (3.56)

*Optimum concentration of DIO was used from reported optimized recipes; ref-1[1], ref-2[2] and ref-3[3].
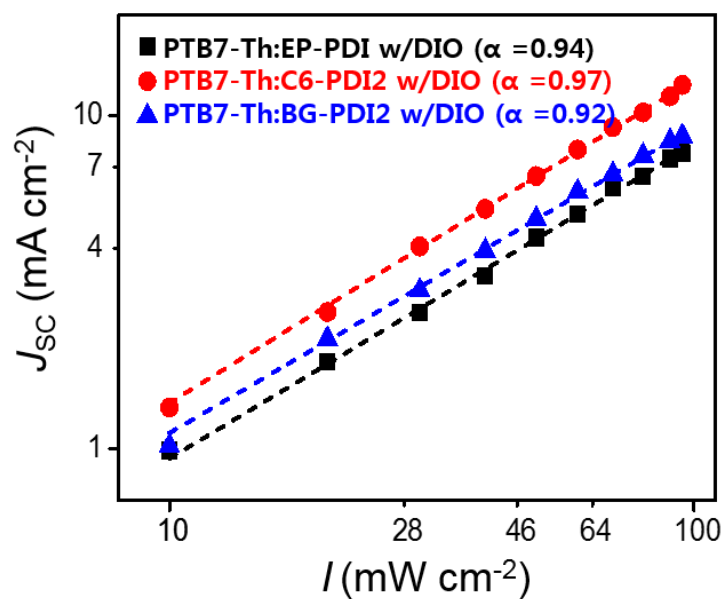
Fig. S3 Light intensity (I) dependent short-circuit current density (J_{SC}) of devices illuminated with simulated solar light (AM 1.5G). Scattered symbols represent experimental data points for devices of PTB7-Th:EP-PDI (squares), PTB7-Th:C6-PDI2 (circles), PTB7-Th:BG-PDI2 (triangles), while the dashed lines demonstrate fits on the data based on the functional $J_{SC} \propto I_{exc}^{a}$. For each system, the value of α as obtained from the fit is reported in the legend.
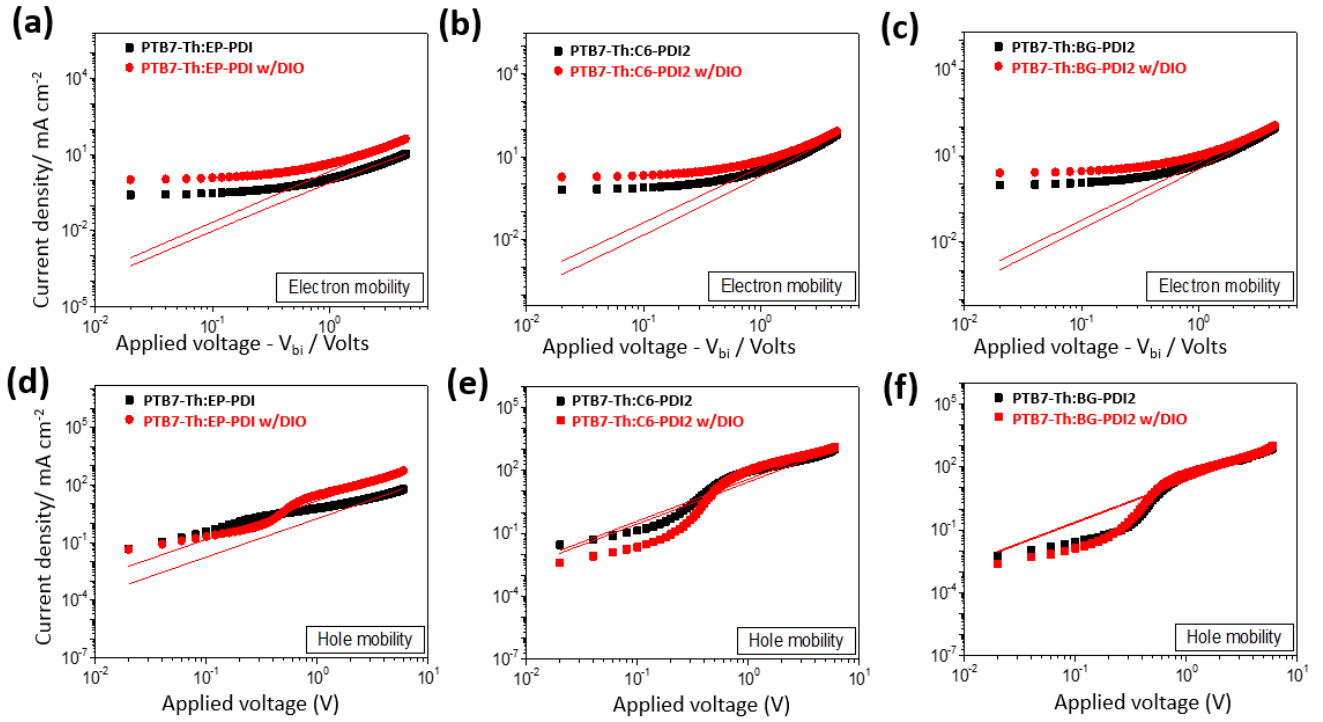
Fig. S4 Dark current density versus voltage ($J - V$) characteristics of (a-c) electron-only devices and (d-f) hole-only devices. The dotted lines are fits based on a modified Mott-Gurney equation that considered the Poole–Frenkel effect. [4]

Table S2. Electron and hole mobility (μ_e and μ_h) extracted from the fitted dark J-V characteristics dsiplayed in Figure S3.

System	μ_e (cm^2 V^{-1} s^{-1})	μ_h (cm^2 V^{-1} s^{-1})
PTB7-Th:EP-PDI	$1.83 \times 10^{-6} \pm 7.32 \times 10^{-7}$	$3.06 \times 10^{-6} \pm 9.89 \times 10^{-7}$
PTB7-Th:EP-PDI2 w/ DIO	$3.67 \times 10^{-6} \pm 1.74 \times 10^{-7}$	$2.54 \times 10^{-5} \pm 2.91 \times 10^{-6}$
PTB7-Th:C6-PDI2	$2.19 \times 10^{-6} \pm 1.41 \times 10^{-6}$	$4.78 \times 10^{-5} \pm 1.54 \times 10^{-6}$
PTB7-Th:C6-PDI2 w/ DIO	$7.05 \times 10^{-6} \pm 3.61 \times 10^{-6}$	$6.85 \times 10^{-5} \pm 2.86 \times 10^{-6}$
PTB7-Th:BG-PDI2	$4.39 \times 10^{-6} \pm 1.57 \times 10^{-6}$	$3.66 \times 10^{-5} \pm 5.53 \times 10^{-6}$
PTB7-Th:BG-PDI2 w/ DIO	$9.57 \times 10^{-6} \pm 3.08 \times 10^{-6}$	$4.15 \times 10^{-5} \pm 3.51 \times 10^{-7}$

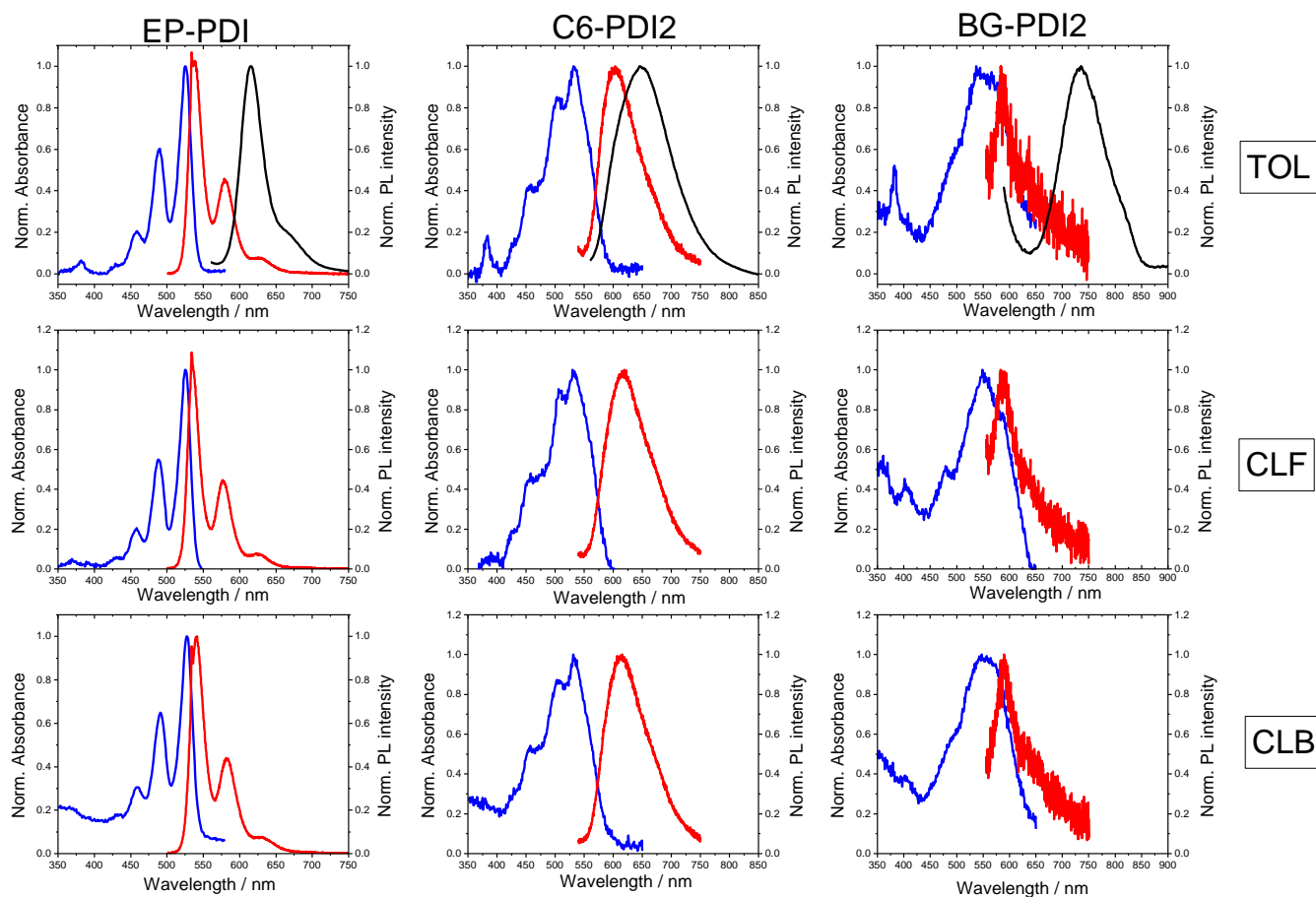**Fig. S5** Comparison of the normalized UV-Vis (blue lines) and PL (red lines) spectra of the three PDI derivatives when measured as dilute solutions in toluene (TOL), chloroform (CLF) and chlorobenzene (CLB), and as thin films developed from toluene solutions (black lines).
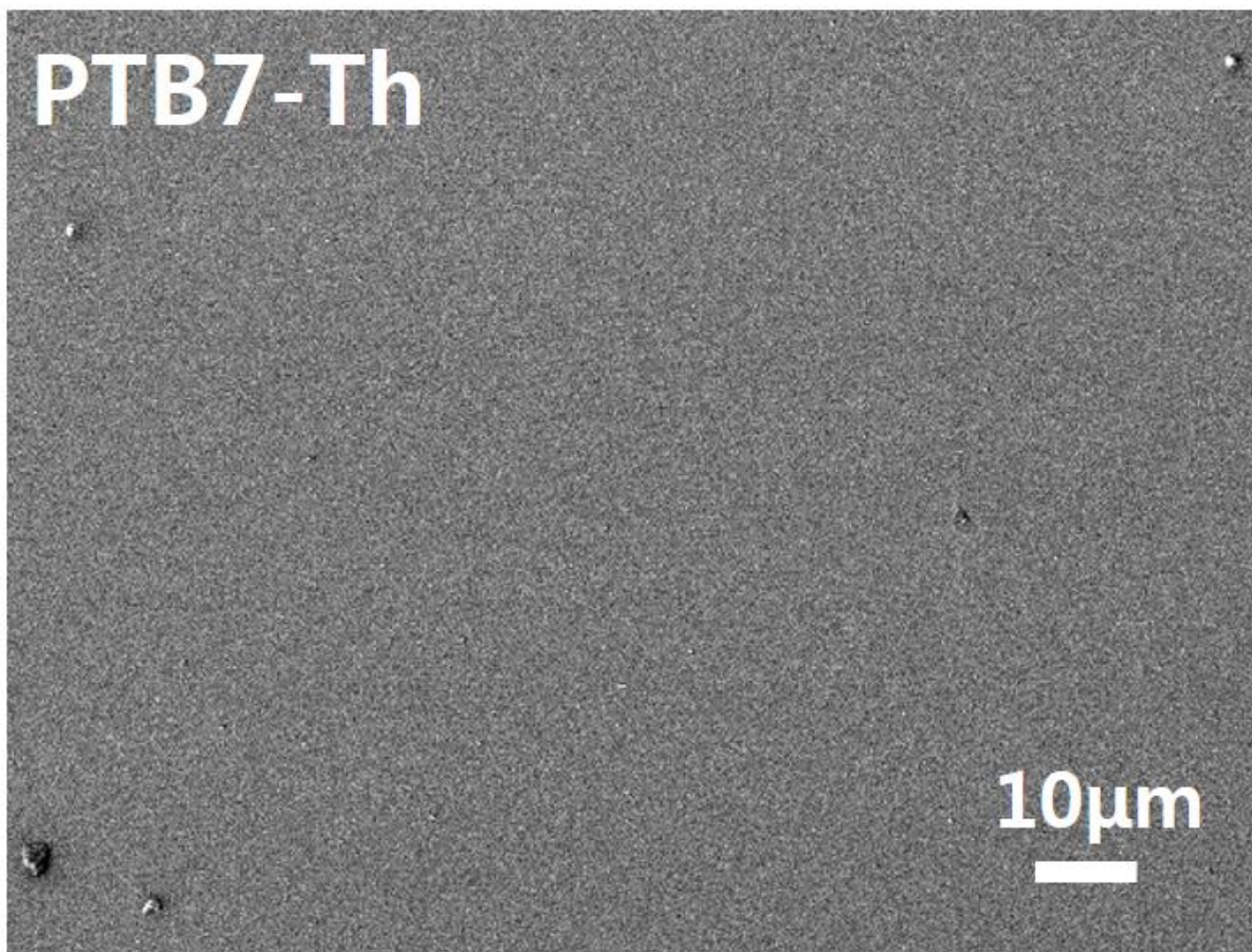
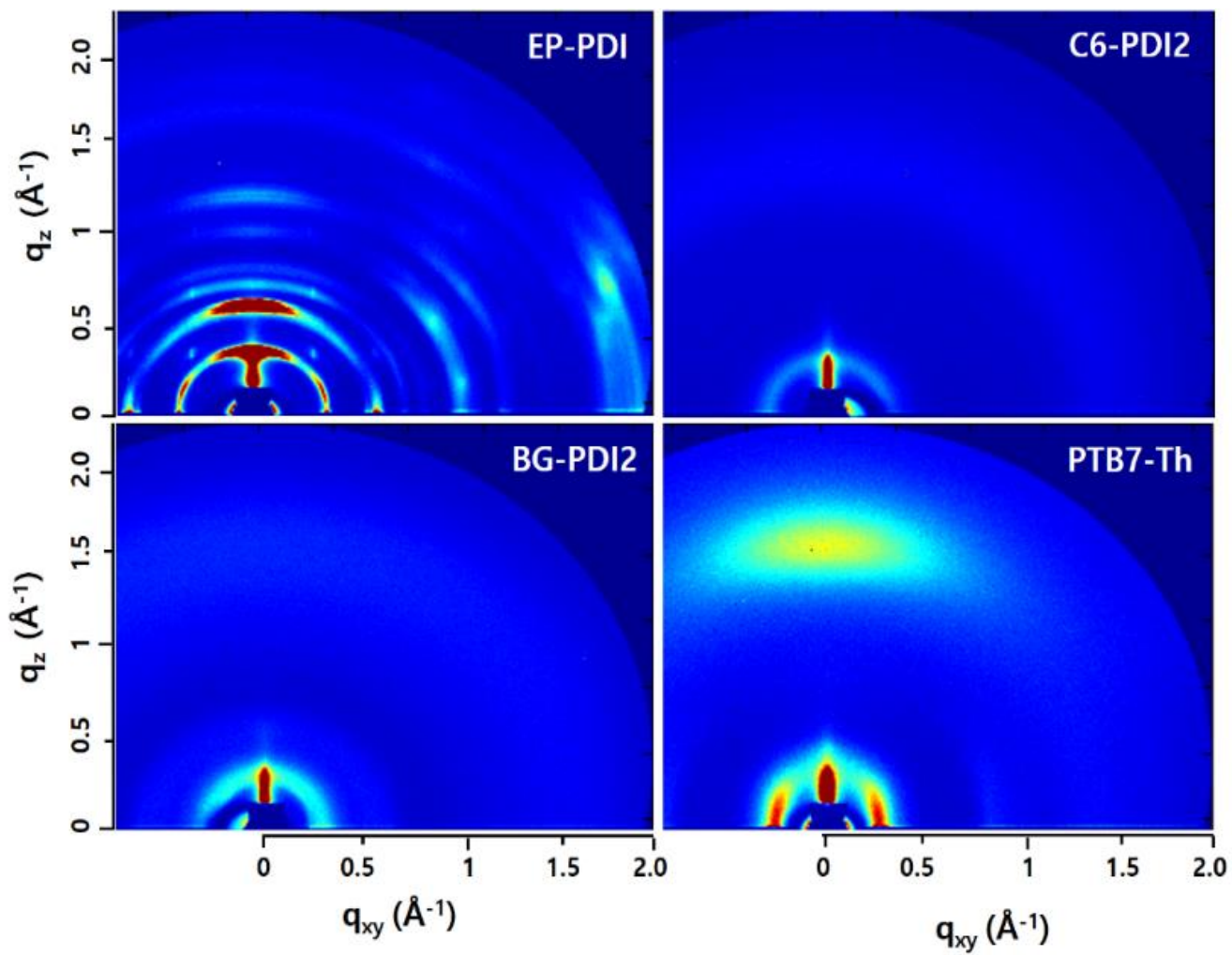**Fig. S6** SEM image of the PTB7-Th neat film.

Fig. S7 2D GIWAXS images of the EP-PDI, C6-PDI2, BG-PDI2 and PTB7-Th pristine films.

Table S3. GIWAXS results for the in-plane scan of the pristine (EP-PDI, C6-PDI2, BG-PDI2 and PTB7-Th) and blend films (PTB7-Th:EP-PDI, PTB7-Th:C6-PDI and PTB7-Th:BG-PDI2 w/ DIO).

	in-plane					in-plane			
pristine films	q (Å^{-1})	d (Å)	FWHM (Å^{-1})	coherence length (nm)	blend films	q (Å^{-1})	d (Å)	FWHM (Å^{-1})	coherence length (nm)
EP-PDI	0.37	17.10	0.03	18.20 ± 0.40	PTB7-Th:EP-PDI	0.27	23.15	0.08	7.25 ± 0.10
	0.40	15.75	2.88	0.20 ± 0.10		0.36	17.40	0.08	6.80 ± 0.20
	0.61	10.25	0.05	12.10 ± 0.20		0.60	10.40	0.09	6.30 ± 0.20
	0.75	8.40	0.03	16.20 ± 2.65		0.61	10.25	0.03	18.40 ± 0.25
	0.85	7.50	0.03	16.80 ± 4.70		0.83	7.60	0.10	5.55 ± 0.40
	1.02	6.15	0.08	7.15 ± 0.25		1.03	6.10	0.08	7.25 ± 0.15
	1.22	5.15	0.06	10.30 ± 0.85		1.22	5.15	0.06	9.95 ± 0.45
	1.71	3.70	0.13	4.50 ± 0.30		1.69	3.70	0.13	4.25 ± 0.25
	1.82	3.45	0.08	7.25 ± 0.85		1.44	4.40	0.12	4.60 ± 1.20
C6-PDI2	0.35	17.80	0.13	4.50 ± 0.05	PTB7-Th:C6-PDI2	0.28	22.20	0.06	9.10 ± 0.10
	1.36	4.70	0.34	1.70 ± 0.20		0.32	19.40	0.14	4.00 ± 0.02
	1.58	4.00	0.30	1.90 ± 0.35		0.84	7.50	0.17	3.30 ± 0.15
						1.31	4.80	0.24	2.35 ± 0.35
						1.44	4.35	0.15	3.75 ± 1.15
						1.60	3.95	0.23	2.50 ± 0.30
BG-PDI2	0.30	21.15	0.13	4.45 ± 0.02	PTB7-Th:BG-PDI2	0.27	23.10	0.06	8.70 ± 0.05
	0.60	10.50	0.13	4.40 ± 0.15		0.32	19.85	0.12	4.60 ± 0.02
	1.27	4.95	0.53	1.10 ± 0.15		0.63	9.90	0.10	5.95 ± 0.30
	1.59	3.95	0.41	1.40 ± 0.15		0.84	7.45	0.10	5.40 ± 0.35
						1.38	4.55	0.42	1.35 ± 0.05
						1.66	3.80	0.21	2.70 ± 0.15
PTB7-TH	0.28	22.75	0.10	5.90 ± 0.05					
	0.85	7.40	0.13	4.30 ± 0.45					
	1.21	5.20	0.30	1.85 ± 1.70					
	1.41	4.45	0.48	1.20 ± 0.60					

Table S4. GIWAXS results for the out-of-plane scan of the pristine (EP-PDI, C6-PDI2, BG-PDI2 and PTB7-Th) and blend films (PTB7-Th:EP-PDI, PTB7-Th:C6-PDI, PTB7-Th:BG-PDI2 w/ DIO).

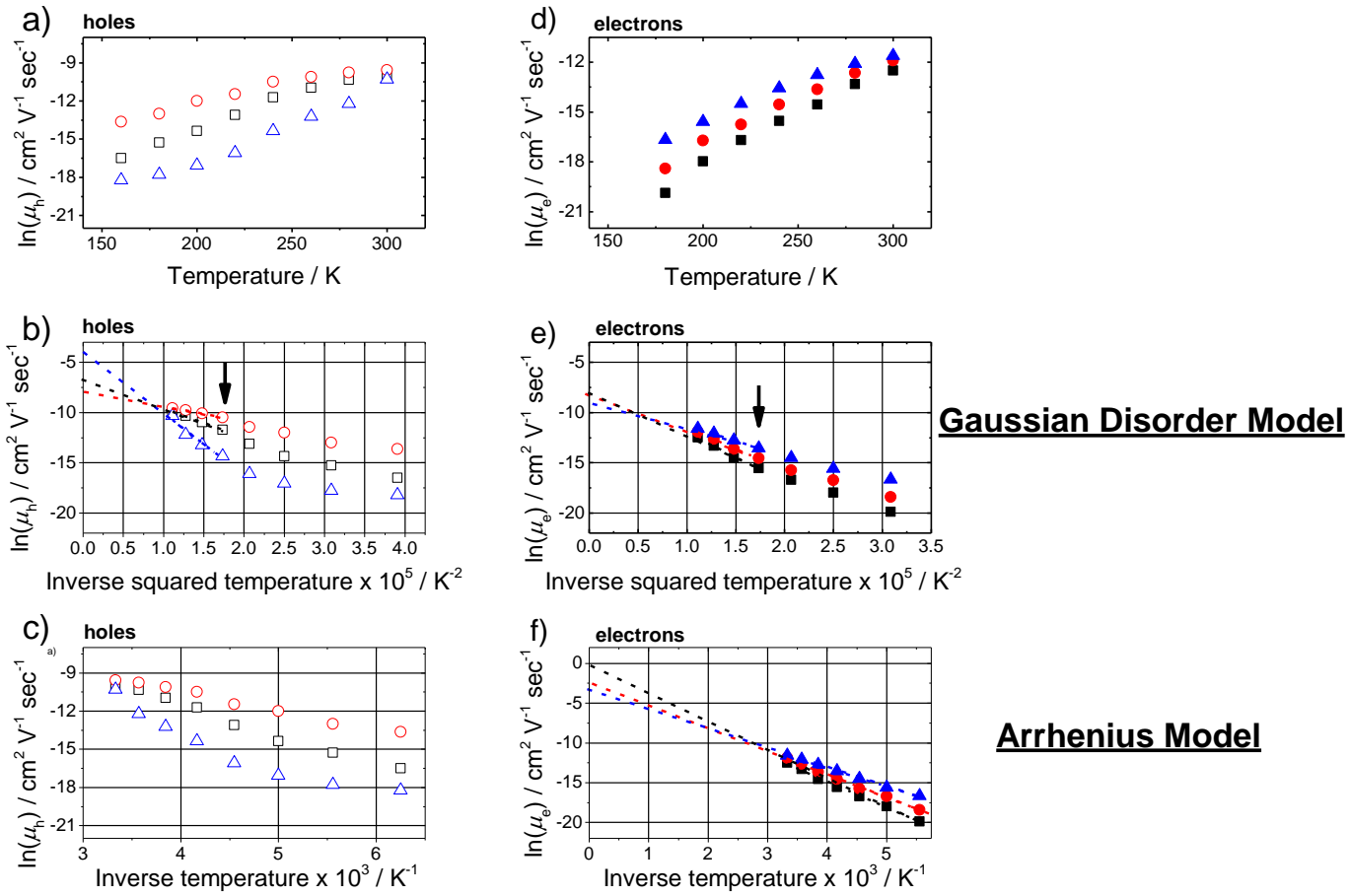| pristine films	out-of-plane				blend films	out-of-plane			
	q (Å^{-1})	d (Å)	FWHM (Å^{-1})	coherence length (nm)		q (Å^{-1})	d (Å)	FWHM (Å^{-1})	coherence length (nm)
EP-PDI	0.35	17.95	0.03	17.25 ± 0.30	PTB7-Th:EP-PDI	0.30	21.00	0.03	17.45 ± 2.00
	0.38	16.70	0.01	38.45 ± 1.70		0.37	17.20	0.04	13.00 ± 0.10
	0.40	15.90	0.03	18.35 ± 2.05		0.64	9.85	0.05	10.40 ± 1.15
	0.64	9.80	0.06	10.15 ± 0.65		0.77	8.15	0.05	11.80 ± 3.60
	0.66	9.60	0.02	33.45 ± 1.00		0.87	7.25	0.05	11.30 ± 1.10
	0.67	9.35	0.01	39.80 ± 1.25		1.07	5.90	0.07	8.50 ± 0.10
	0.77	8.20	0.06	9.25 ± 0.6		1.25	5.00	0.09	6.55 ± 0.15
	0.86	7.30	0.07	8.45 ± 0.45		1.47	4.25	0.17	3.25 ± 0.25
	1.06	5.90	0.07	8.45 ± 0.15		1.69	3.70	0.26	2.20 ± 0.35
	1.26	5.50	0.08	7.10 ± 0.05		1.87	3.40	0.15	3.80 ± 1.10
	1.69	3.70	0.10	5.90 ± 0.30					
	1.84	3.40	0.19	3.00 ± 0.20					
C6-PDI2	0.30	20.95	0.08	7.30 ± 0.20	PTB7-Th:C6-PDI2	0.29	21.85	0.04	15.65 ± 0.90
	1.46	4.30	0.52	1.10 ± 0.01		0.92	6.85	0.32	1.80 ± 0.20
						1.47	4.30	0.52	1.10 ± 0.20
						1.66	3.80	0.41	1.35 ± 0.30
BG-PDI2	0.30	20.90	0.09	6.60 ± 0.30	PTB7-Th:BG-PDI2	0.30	21.20	0.06	9.00 ± 0.40
	1.54	4.10	0.62	0.90 ± 0.01		0.65	9.70	0.14	3.90 ± 0.50
						1.24	5.05	0.44	1.30 ± 0.04
						1.63	3.85	0.40	1.40 ± 0.02
PTB7-Th	0.48	13.05	0.09	6.35 ± 0.30					
	1.60	3.95	0.39	1.45 ± 0.01					

Fig. S8 Overview of the mobility dependence on temperature, both for electrons and holes, for all three device systems studied. The dependence is illustrated as dependence on i) T, ii) T^{-2}, when the GDM model is used, and iii) T^{-1} when the Arrhenius model is used. a) – c) hole mobilities (open symbols), and d) – f) electron mobilities (filled symbols) of PTB7-Th:EP-PDI (black squares), PTB7-Th:C6-PDI2 (red circles) and PTB7-Th:BG-PDI2 (blue triangles). The point arrows in b) and e) indicate the turnover temperature $T_d = 240$ K, where a transition from dispersive to non-dispersive transport takes place. The GDM formalism was applied for temperatures higher than T_d.

References

1. R. Singh, E. Aluicio-Sarduy, Z. Kan, T. Ye, R. C. I. MacKenzie and P. E. Keivanidis, *Journal of Materials Chemistry A*, 2014, **2**, 14348-14353.
2. R. Singh, J. Lee, M. Kim, P. E. Keivanidis and K. Cho, *Journal of Materials Chemistry A*, 2017, **5**, 210-220.
3. X. Zhang, Z. Lu, L. Ye, C. Zhan, J. Hou, S. Zhang, B. Jiang, Y. Zhao, J. Huang, S. Zhang, Y. Liu, Q. Shi, Y. Liu and J. Yao, *Advanced Materials*, 2013, **25**, 5791-5797.
4. T. Ye, R. Singh, H.-J. Butt, G. Floudas and P. E. Keivanidis, *ACS Applied Materials & Interfaces*, 2013, **5**, 11844-11857.